

## Raman scattering spectra of superconducting $\text{Bi}_2\text{Sr}_2\text{CaCu}_2\text{O}_8$ single crystals

D. Kirillov

Varian Research Center, 611 Hansen Way, Palo Alto, California 94303

I. Bozovic, T. H. Geballe, A. Kapitulnik, and D. B. Mitzi

Department of Applied Physics, Stanford University, Stanford, California 94305-4090

(Received 12 September 1988)

Raman spectra of  $\text{Bi}_2\text{Sr}_2\text{CaCu}_2\text{O}_8$  single crystals with superconducting phase-transition temperature of 90 K have been studied. The spectra contained phonon lines and electronic continuum. Phonon energies and polarization selection rules were measured. A gap in the electronic continuum spectrum was observed in a superconducting state. Noticeable similarity between Raman spectra of  $\text{Bi}_2\text{Sr}_2\text{CaCu}_2\text{O}_8$  and  $\text{YBa}_2\text{Cu}_3\text{O}_7$  was found.

Raman scattering provides important information on phonon spectra and low-energy electronic spectra of superconductors.<sup>1</sup> In the present work, we applied Raman scattering to study the new high-temperature superconductor  $\text{Bi}_2\text{Sr}_2\text{CaCu}_2\text{O}_8$ .<sup>2</sup> The single-crystal samples used for the study were prepared by mixing powders of  $\text{Bi}_2\text{O}_3$ ,  $\text{SrCO}_3$ ,  $\text{CaCO}_3$ , and  $\text{CuO}$  and melting them in a crucible containing nucleation sites. The temperature gradient of 20°C over the crucible was maintained, and the cooling rate of 0.7°C/min was used. Shiny black crystals with faces as large as 1×1 cm which could be easily cleaved parallel to the  $ab$  plane were obtained. Additional details on the preparation of the crystals are given in Ref. 3. A rotating anode four circle Huber x-ray diffractometer was utilized to determine the structure and to orient the crystals. Diffractograms showed very narrow peaks which were indexable by a  $5.42 \times 5.42 \times 30.89$ -Å unit cell with a superstructure along the  $b$  axis. This superstructure makes the unit-cell dimension in the  $b$  direction equal to  $\approx 27$  Å, and the proper symmetry point group for the structure is not tetragonal, but, most likely, orthorhombic  $D_{2h}$ .<sup>4</sup> The four-point resistance measurements showed typically a 1-K-wide transition to zero resistance at  $T_c = 90$  K. Magnetization measurements were performed with a Quantum Design SQUID magnetometer. A large and strongly orientation-dependent diamagnetic signal has been observed at low temperatures, with an onset at 94 K. Low-energy electron diffraction studies of cleaved samples<sup>5,6</sup> verified that the surface structure of those compounds was identical to the bulk structure, in particular with respect to the superstructure. The same results were obtained using ultraviolet and x-ray spectroscopy.

The Raman spectra were taken in backscattering geometry using 514.5- or 488.0-nm radiation of an argon laser as an excitation source. The spectra were analyzed by a triple scanning Spex spectrometer. During low-temperature measurements the sample was in vacuum attached by a thermoconducting paste to a cold finger of a He cryostat. The sample was a  $3 \times 5 \times 0.5$  mm platelet with the larger facets parallel to the  $ab$  plane. The density of the excitation radiation was kept low in order to prevent heating and optical damage of the sample.

The room-temperature polarized Raman spectra are

shown in Fig. 1. The scattering configuration is defined by symbols such as  $z(xx)\bar{z}$ , which means that the incident light propagates along the  $z$  axis and is polarized along the  $x$  axis, and the scattered light is polarized along the  $x$  axis and propagates in the opposite direction along the  $z$  axis. The axes  $x, y, z$  are chosen along the axes  $a, b, c$  of the crystallographic unit cell, correspondingly. As can be seen from Fig. 1, the spectrum consists of an electronic continuum and discrete phonon lines and is quite similar

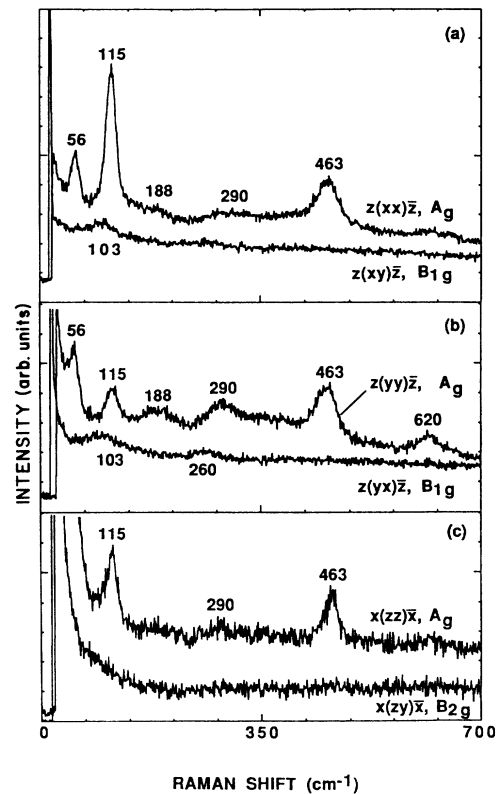


FIG. 1. Raman spectrum of  $\text{Bi}_2\text{Sr}_2\text{CaCu}_2\text{O}_8$  single crystal,  $T = 300$  K. Polarization configurations and corresponding symmetry types of phonons active in scattering are shown. Excitation by a 514.5-nm laser line.

to that of  $\text{YBa}_2\text{Cu}_3\text{O}_7$ . As in the case of  $\text{YBa}_2\text{Cu}_3\text{O}_7$  (see, for example, Refs. 7 and 8), the spectrum is strongest in  $xx$ ,  $yy$ , and  $zz$  polarizations and corresponds mainly to totally symmetric  $A_g$  irreducible representation of the  $D_{2h}$  point group. The dominant phonon features of the two compounds are similar: 54, 115, 292, and  $467\text{ cm}^{-1}$  in  $\text{Bi}_2\text{Sr}_2\text{CaCu}_2\text{O}_8$  to compare with 112, 150, 335, and  $499\text{ cm}^{-1}$  in  $\text{YBa}_2\text{Cu}_3\text{O}_7$ . The Raman spectrum of a  $\text{Bi}_2\text{Sr}_2\text{CaCu}_2\text{O}_8$  film prepared by electron-beam evaporation on  $\text{SrTiO}_3$  substrates is shown in Fig. 2. The  $550\text{--}620\text{-cm}^{-1}$  doublet, which can be an analog of the  $590\text{--}640\text{ cm}^{-1}$  doublet in  $\text{YBa}_2\text{Cu}_3\text{O}_7$ , is noticeably stronger in epitaxial thin films (Fig. 2) than in the single crystal, Fig. 1. The similarity between the spectra of  $\text{Bi}_2\text{Sr}_2\text{CaCu}_2\text{O}_8$  and  $\text{YBa}_2\text{Cu}_3\text{O}_7$  suggests that the strongest features in the spectra of both materials originate predominantly from vibrations of similar Cu-O planar complexes present in both materials.

Our results on the symmetry of phonons can be summarized as follows:  $A_g$ -type phonons, 53, 115, 188 (weak), 291, 360 (weak), 463, and  $620\text{ cm}^{-1}$ ;  $B_{1g}$ -type phonons, 103 (weak) and  $260\text{ cm}^{-1}$  (weak). As can be seen from the comparison of  $z(xx)\bar{z}$  and  $z(yy)\bar{z}$  spectra the material is markedly anisotropic in  $xy$  plane which is manifested in different  $xx$  and  $yy$  scattering tensor components for  $A_g$  phonons. The  $yy$  components correspond to the case when the incident and scattered light are polarized along the direction of the superstructure. Note, however, that as in the case of  $\text{YBa}_2\text{Cu}_3\text{O}_7$ ,<sup>7</sup> resonant Raman scattering may introduce strong changes in the selection rules, and the interpretation of phonon lines based mainly on the experimentally observed selection rules should be accepted with caution. The resonance Raman behavior is quite different for  $xx$  and  $yy$  components, as can be seen by comparing Fig. 1 (514.5-nm excitation) and Fig. 3 (488.0-nm excitation). While the  $z(xx)\bar{z}$  spectra are quite similar for both excitation wavelengths, the  $z(yy)\bar{z}$  spectra differ noticeably. The intensity of the  $463\text{-cm}^{-1}$  line grows resonantly in relation to other lines in the  $z(yy)\bar{z}$  spectrum. The Fano-type interference between the electronic continuum and the  $290\text{-cm}^{-1}$  phonon line which is hardly seen in Fig. 1 becomes apparent in the  $z(yy)\bar{z}$  spectrum of Fig. 3. The asymmetric cut off of the line is on the low-energy

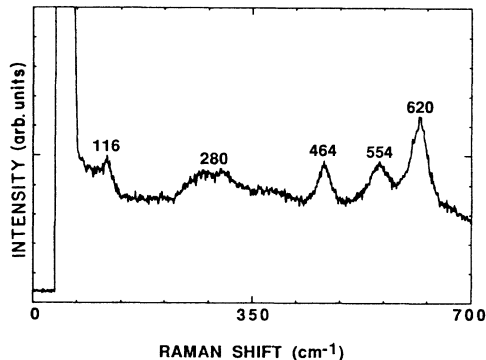


FIG. 2. Raman spectrum of  $\text{Bi}_2\text{Sr}_2\text{CaCu}_2\text{O}_8$  thin film grown on  $\text{SrTiO}_3$  substrate. Notice the strong growth of the intensity of the  $550\text{--}620\text{-cm}^{-1}$  doublet in the spectrum of a thin film.

side, while it is on the high-energy side in  $\text{YBa}_2\text{Cu}_3\text{O}_7$ ,<sup>8</sup> which indicates that Fano coupling coefficients in  $\text{YBa}_2\text{Cu}_3\text{O}_7$  and  $\text{Bi}_2\text{Sr}_2\text{CaCu}_2\text{O}_8$  have opposite signs.

Our data can be compared with recently published Raman phonon spectra of  $\text{Bi}_2\text{Sr}_2\text{CaCu}_2\text{O}_8$ .<sup>9,10</sup> While our phonon spectra have practically no common features with data for polycrystalline samples,<sup>9</sup> they are quite similar to the data of Ref. 10 for single crystals. In addition, they contain some new information. We were able to observe the low-energy phonon line at  $56\text{ cm}^{-1}$  and to measure the  $x(zz)\bar{x}$  and  $x(zy)\bar{x}$  spectra, which are difficult to measure due to the layered structure of the material. We also identified the Fano-type interference effects for the  $290\text{-cm}^{-1}$  line. The highest-energy phonon line is at  $620\text{ cm}^{-1}$  in our samples, while it is at  $\approx 640\text{ cm}^{-1}$  in the spectra of Ref. 10.

The low-temperature spectrum is shown in Fig. 4. Scattering was measured along the  $z$  axis. The sample with the highest surface quality of the  $xy$  plane, but unoriented in this plane, was studied. As can be seen from the spectrum, a steplike depression below  $290\text{ cm}^{-1}$  is present in the low-energy part of the electronic spectrum at 20 K, which practically disappears at the temperature of the superconducting phase transition,  $T=90\text{ K}$ . This steplike feature is expected to occur in a superconductor with a gap.<sup>1</sup> As can be seen from Fig. 4(b), the intensity of electronic scattering is not equal to zero within the superconducting gap. This may be partly due to weak parasitic radiation which is very difficult to eliminate completely in low temperature Raman measurements. The shape of the superconducting gap scattering spectrum can be evaluated by dividing the spectrum of Fig. 4(b) by the spectrum of Fig. 4(a) and subtracting the temperature-independent contribution. The resulting spectrum is

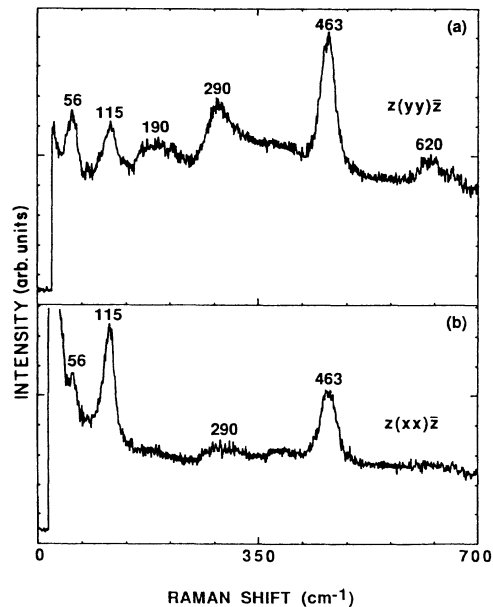


FIG. 3. Raman spectrum  $\text{Bi}_2\text{Sr}_2\text{CaCu}_2\text{O}_8$  single crystal excited by a 488.0-nm laser line. Notice the enhancement of the  $463\text{-cm}^{-1}$  line in the  $z(yy)\bar{z}$  spectrum and marked appearance of the Fano-type line shape for the  $290\text{-cm}^{-1}$  line.

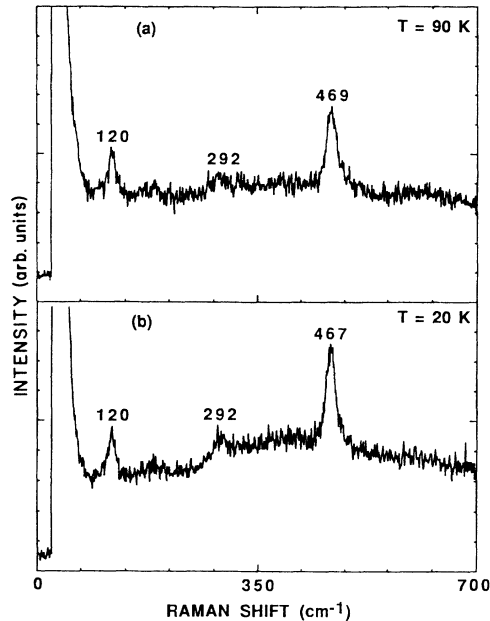


FIG. 4. Unpolarized Raman spectra of  $\text{Bi}_2\text{Sr}_2\text{CaCu}_2\text{O}_8$  single crystals (a) at the temperature of the superconducting phase transition  $T=90$  K and (b) in a superconducting state at  $T=20$  K. The depression of electronic scattering continuum in the low-energy part of the spectrum in a superconducting state, spectrum (b), corresponds to the formation of a superconducting gap.

shown in Fig. 5. Due to broadening of the gap feature, scattering within the gap, contributions of anisotropy, phonons, and disorder, it is difficult to obtain the value of the gap from the spectrum. There is no suitable theoretical treatment of the problem. If we take the gap to be approximately equal to the low-energy boundary of the step,

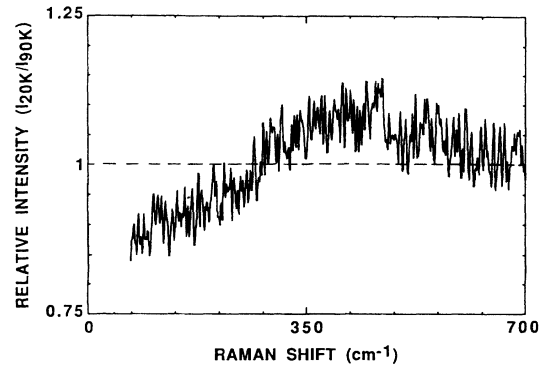


FIG. 5. The shape of the superconducting gap scattering spectrum. It is obtained dividing the spectrum of Fig. 4(b) by the spectrum of Fig. 4(a) and subtracting the temperature-independent background.

as it is done for the infrared absorption in superconductors with short correlation length,<sup>11</sup> we obtain  $2\Delta \approx 260 \text{ cm}^{-1} \approx 32 \text{ meV} \approx 4kT_c$ . If the energy of the broad maximum in the scattering intensity, which might represent the pile up of the electronic states in a superconductor, is taken as the value of the gap,<sup>1</sup> we obtain  $2\Delta \approx 450 \text{ cm}^{-1} \approx 56 \text{ MeV} \approx 7kT_c$ . A similar value for the gap was obtained using electron tunneling spectroscopy on single-crystal samples grown in the same crucible as our samples.<sup>12</sup>

In conclusion, Raman scattering spectra of  $\text{Bi}_2\text{Sr}_2\text{CaCu}_2\text{O}_8$  were measured. Strongest phonon lines were observed only in parallel polarizations indicating  $A_g$ -type modes. A superconducting gap appeared in low-temperature spectra. Strong similarity between electronic and phonon spectra of  $\text{Bi}_2\text{Sr}_2\text{CaCu}_2\text{O}_8$  and  $\text{YBa}_2\text{Cu}_3\text{O}_7$  was observed.

<sup>1</sup>M. V. Klein and S. B. Dierker, *Phys. Rev. B* **29**, 4976 (1984).

<sup>2</sup>H. Maeda, Y. Tanaka, M. Fukutomi, and T. Asano, *Jpn. J. Appl. Phys. Lett.* **27**, L209 (1988).

<sup>3</sup>D. B. Mitzi, P. Feller, T. H. Geballe, and A. Kapitulnik (unpublished).

<sup>4</sup>M. A. Subramanian, C. C. Torardi, J. C. Calbrese, J. Gopkrishnan, K. J. Morrissey, T. R. Askew, R. B. Flippen, U. Chowdry, and A. W. Sleight, *Science* **239**, 1015 (1988).

<sup>5</sup>P. A. P. Lindberg, Z. X. Shen, D. B. Mitzi, I. Lindau, W. E. Spicer, and A. Kapitulnik, *Nature* (to be published).

<sup>6</sup>Z. X. Shen, P. A. P. Lindberg, B. O. Wells, D. B. Mitzi, I. Lindau, W. E. Spicer, and A. Kapitulnik, this issue, *Phys. Rev. B* **38**, 11 820 (1988).

<sup>7</sup>D. Kirillov, I. Bozovic, K. Char, and A. Kapitulnik (unpublished).

<sup>8</sup>S. L. Cooper, M. V. Klein, B. G. Pazol, J. P. Rice, and T. J. Negran, *Phys. Rev. B* **37**, 5920 (1988).

<sup>9</sup>L. A. Farrow, L. H. Greene, J. M. Tarascon, P. A. Morris, W. A. Bonner, and G. W. Hull, *Phys. Rev. B* **38**, 752 (1988).

<sup>10</sup>M. Cardona, C. Thomsen, R. Liu, H. G. von Schnering, and M. Hartweg, *Solid State Commun.* **66**, 1225 (1988).

<sup>11</sup>M. Tinkham, *Introduction to Superconductivity* (McGraw-Hill, New York, 1975).

<sup>12</sup>M. Lee, D. B. Mitzi, A. Kapitulnik, and M. R. Beasley, *Phys. Rev. B* (to be published).